COLLISIONS BETWEEN PLANETESIMLAS IN THE GRAVITY REGIME WITH iSALE CODE.

R. Suetsugu[1], H. Tanaka[2], H. Kobayashi[3], H. Genda[4], [1]School of Medicine, University of Occupational and Environmental Health (Iseigaoka, Yahatanishi-ku, KitaKyushu, 807-8555, Japan, ryos@med.uoeh-u.ac.jp), [2]Astronomical Institute, Tohoku University (Aramaki, Aoba-ku, Sendai, 980-8578, Japan), [3]Department of Physics, Graduate School of Science, Nagoya University (Furo-cho, Chikusa-ku, Nagoya, 464-8602, Japan), [4]Earth-Life Science Institute, Tokyo Institute of Technology (Ookayama, Meguro-ku, Tokyo, 152-8550, Japan) .

Introduction: Collisions are one of the most important processes in planet formation, because planetary bodies in the Solar System are thought to have experienced a lot of collisions in accretion process. Thus, collisional processes have been examined extensively. Collisional outcomes are characterized by the specific impact energy Q_R [1]. Especially, Q_R required to disperse the largest body having exactly half the total mass after the collision is called the critical specific impact energy Q_{RD}^*. Typically, in the case of $Q_R > Q_{RD}^*$, collisions between planetesimals are regarded as disruptive collisions, while they are erosive collisions when $Q_R << Q_{RD}^*$.

The values of Q_{RD}^* in the gravity regime have been investigated by several impact simulations [1-5]. These impact simulations showed the dependence of the values of Q_{RD}^* on impact conditions. For example, the value of Q_{RD}^* increase monotonically with increasing the target size, because collisional fragments are more easily bound by the gravitational force of the target. The critical specific impact energy also depends on the physical properties of the target (e.g. material strength, porosity, and friction). Especially, the friction significantly dissipates impact energy, which tends to hinder the disruption of the target [4]. In such a case, the values of Q_{RD}^* reach about 10 times the values of Q_{RD}^* without the friction. Moreover, recent impact simulations show that Q_{RD}^* depend not only on the impact conditions but also on numerical resolutions [5]. Genda et al. (2015) [5] performed SPH simulation at various numerical resolutions and showed that the values of Q_{RD}^* obtained by the high resolution are rather lower than the case of low resolution.

Although the improvement of numerical simulation helped us our understanding of properties of the critical specific impact energy, it also caused some confusion. For example, there are variations in the value of Q_{RD}^* for constant target size by up to a factor of 10. The variations in the values of Q_{RD}^* would have significant influence on planet formation, because the mass of formed protoplanets is proportional to $(Q_{RD}^*)^{0.87}$ [6]. Thus, values of Q_{RD}^* obtained by several impact simulations are needed to be organized.

In this study, we examine the collision between planetesimals and provide constraint on the critical specific impact energy in the gravity regime. We perform high resolution impact simulation by using shock-physics code, iSALE-2D [7-9].

Numerical Methods: We examine the disruptive collision between planetesimals, using shock-physics code, iSALE-2D, the version of which is iSALE-Chicxulub [7-9]. In our simulation, we use the Tillotson equation of state for basalt which has been widely applied in other previous studies including planet- and planetesimal-size collisional simulations. Although the Tillotson parameters for basalt of the iSALE-2D are set to experimental values, we used the parameter sets of basalt referenced in previous studies.

We employ the two-dimensional cylindrical coordinate system and perform head-on impact simulations between two planetesimals. We assumed that planetesimals are not differentiated. Also, planetesimals are assumed to be composed of basalt. Basically, the impact velocity of impactor planetesimals is fixed at 3 km/s. To carry on impact simulations with a wide range of impact energy, we changed the size of the impactor. We consider four cases with the number of cells per target radius n_{tar} = 100, 200, 400, and 800. Then, the values of the spatial cell size for each numerical resolution n_{tar}=100, 200, 400, and 800 are 1000, 500, 250, and 125 m, respectively. The self-gravity is calculated by the algorithm in iSALE-2D based on a Barnes-Hut type algorithm, which can reduce the computational cost of updating the gravity field. The iSALE-2D can deal with the effects of strength, damage, and porosity. However, in this study, we do not consider such an effect in order to compare outcomes of high resolution SPH simulation [5].

Results: Fig.1 shows an example of snapshot of head-on impact simulation. The color contour represents the specific kinetic energy. If the specific kinetic energy of cells is larger than the gravitational potential energy of the largest body formed by collision, we regard cells as ejecta.

Fig. 2 shows ejected mass for various numerical resolutions as a function of the impact energy. The ejected mass normalized by the total mass. Asterisks, squares, triangles, and circles represent the cases with n_{tar} =100, 200, 400, and 800, respectively. In all the cases shown in Fig. 2, the ejected mass increases with increasing impact energy. We find that the amount of the ejecta for each impact energy increases with increasing numerical resolution. We also find that the differences in the values of M_{ej}/ M_{tot} between numerical resolutions become smaller in the case of high resolution.

In Fig. 2, the vertical dashed lines represent the critical specific impact energy Q_{RD}^*. Based on linear interpolation of the two data sets of Q_R across M_{ej}/ M_{tot} =0.5, we estimated Q_{RD}^*=24.5, 21.3, 19.8 and 19.1 kJ/kg for n_{tar}=100, 200, 400, and 800, respectively. Unfortunately, the value of Q_{RD}^* for n_{tar}=800 does not fully converge. However, we confirm that it is close to the converged value estimated by the least-squares fit to Q_{RD}^* for each numerical resolution.

Fig. 3 shows the dependence of the critical specific impact energy for head-on collision on target size. We find that the values of the critical specific impact energy estimated by this study become rather low as compared with those obtained by some previous studies [1-3]. However, our results are roughly consistent with the values of Q_{RD}^* by performing with very-high resolution simulations [5], although their numerical method is different from ours. Thus, it seems that the dependence of Q_{RD}^* on numerical methods becomes small in the case of hyper numerical resolution.

We will also discuss the erosive collisions in the gravity regime, and compare our results with previous studies.

Acknowledgements: We appreciate the developers of iSALE, including G. Collins, K. Wünnemann, B. Ivanov, J. Melosh, and D. Elbeshausen.

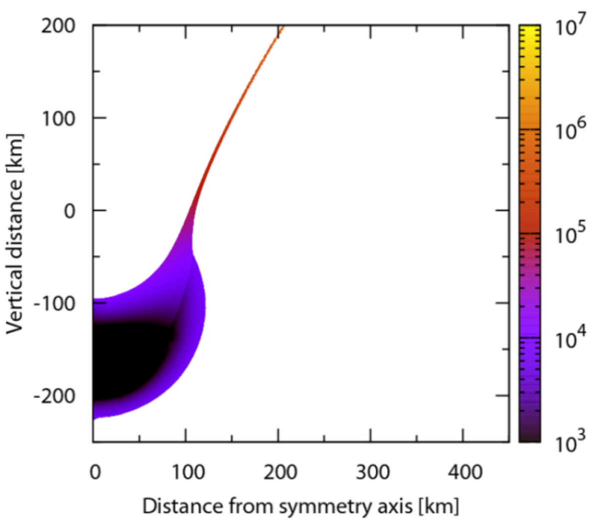

Figure 1: Example of a snapshot of simulation of head-on impact between a target (100km) and an impactor (16 km) in the case of n_{tar}=800. Color contour represents the specific kinetic energy.

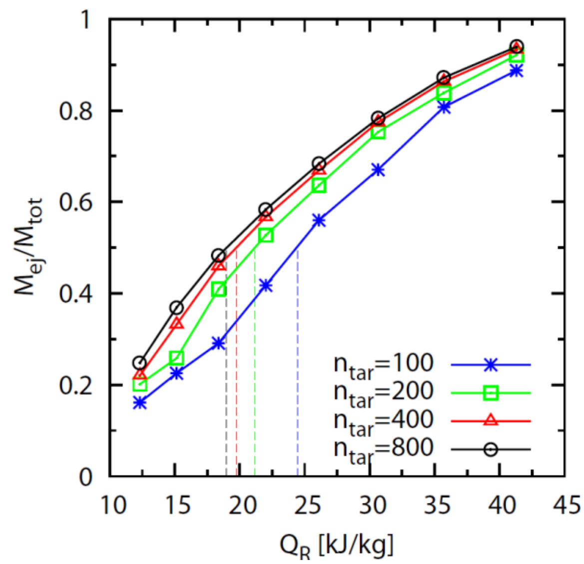

Figure 2: Ejected mass normalized by total mass (M_{ej}/ M_{tot}) as a function of Q_R. Asterisks, squares, triangles, and circles represent the calculations with n_{tar}=100, 200, 400, and 800, respectively. The vertical dashed lines represent Q_{RD}^* for the above four cases.

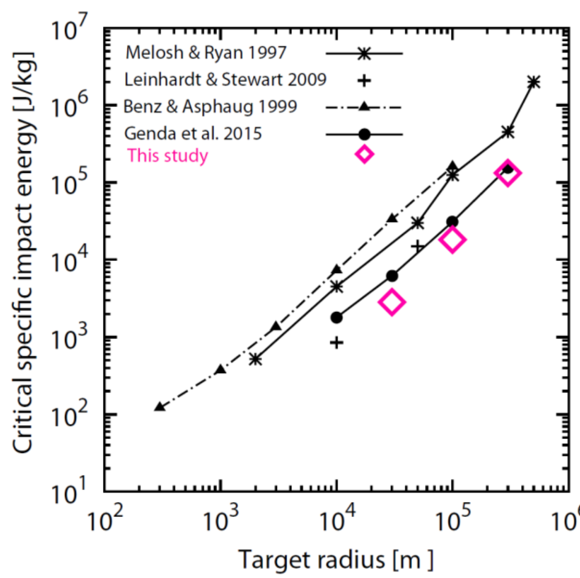

Figure 3: Critical specific impact energy as a function of target radius in the case of head-on collision. Diamond marks represent our results, and other marks are results obtained by various previous works.

References: [1] Leinhardt, Z. M. and Stewart, S. T., (2009), *Icarus*, 199, 542. [2] Benz, W. and Asphaug, E., (1999), *Icarus*, 142, 5. [3] Melosh, H.J., Ryan, E.V., (1997), *Icarus*, 129, 562 [4] Jutzi, M., (2015), *Planet. Space Sci.* 107, 3. [5] Genda, H. et al., (2015), *Icarus*, 262, 58. [6] Kobayashi, H. and Tanaka, H., (2010), *Icarus*, 206, 735 [7] Amsden A. A., et al. (1980) *LANL Report*, LA-8095. 101. [8] Ivanov B. A., et al. (1997), *IJIE*, 20, 411. [9] Wünnemann, K., et al. (2006), *Icarus*, 180, 514.